

DOI: 10.1002/adfm.200600818

# Multifunctional Micelles for Cancer Cell Targeting, Distribution Imaging, and Anticancer Drug Delivery\*\*

By Chun-Kai Huang, Chun-Liang Lo, Hung-Hao Chen, and Ging-Ho Hsiue\*

Multifunctional micelles for cancer cell targeting, distribution imaging, and anticancer drug delivery were prepared from an environmentally-sensitive graft copolymer, poly(*N*-isopropyl acrylamide-*co*-methacryl acid)-*g*-poly(*D,L*-lactide) (P(NIPAAm-*co*-MAAc)-*g*-PLA), a diblock copolymer, methoxy poly(ethylene glycol)-*b*-poly(*D,L*-lactide) (mPEG-PLA) and two functionalized diblock copolymers, galactosamine-PEG-PLA (Gal-PEG-PLA) and fluorescein isothiocyanate-PEG-PLA (FITC-PEG-PLA). Anticancer drug, free base doxorubicin (Dox) was incorporated into the inner core of multifunctional micelles by dialysis. From the drug release study, a change in pH (from pH 7.4 to 5.0) deformed the structure of the inner core from that of aggregated P(NIPAAm-*co*-MAAc), causing the release of a significant quantity of doxorubicin (Dox) from multifunctional micelles. Multifunctional micelles target specific tumors by an asialoglycoprotein (HepG2 cells)-Gal (multifunctional micelle) receptor-mediated tumor targeting mechanism. This mechanism then causes intracellular pH changes which induce Dox release from multifunctional micelles and that micelles have strong effects on the viability of HepG2 cells and are abolished by galactose. Confocal laser scanning microscopy (CLSM) reveals a clear distribution of multifunctional micelles. With careful design and sophisticated manipulation, polymeric micelles can be widely used in cancer diagnosis, cancer targeting, and cancer therapy simultaneously.

## 1. Introduction

Research on multicomponent micelles for biomedical applications has generally shown that virtually all types and classes of micelles exhibit beneficial properties, such as specific functionality, enhanced specific tumor targeting, stabilized nanostructures, overcame defects from various materials, and displayed multifunctions.<sup>[1–4]</sup> In the polymer field, multicomponent micelles (also called mixed micelles) have been widely investigated in di-diblock copolymer, di-triblock copolymer, tri-triblock copolymer, and graft-diblock copolymer systems.<sup>[2–10]</sup> Over the last decade, most studies were concerned with micellization theories of mixed micelles.<sup>[5–10]</sup> However, few studies examine drug delivery.<sup>[3,4]</sup> Mixed micelles are quite complicated, and the complete core-shell structure cannot be observed clearly. This creates a bottleneck in biomedical applications.

The authors of this study present micellization results not offered by other mixed micelle studies. In principle, it is possible to make clusters by mixing graft copolymer and diblock copolymer in aqueous solution. This study presents a multifunctional micelle encapsulating doxorubicin (Dox), an anticancer drug. The micelle was prepared by dialysis from a graft copolymer, a diblock copolymer and two functionalized diblock copolymers, as shown in Figure 1. This type of multifunctional micelle has several important advantages over other particulate drug delivery systems. These advantageous characteristics include the ability to overcome some limitations in ionic charge materials in drug delivery,<sup>[4]</sup> easy dialysis-method preparation,<sup>[4]</sup> better control of particle size and particle distribution for suitable physiological conditions, easy modification for displaying functionalities (e.g., specific tumor targeting or fluorescent imaging for micellar distribution), stimulus-response behavior for drug release control (e.g., charge in volume in response to a change in pH, ionic strength or temperature), and the ability to use a single polymeric micelle for multiple purposes.

## 2. Results and Discussion

First, a graft copolymer poly(*N*-isopropyl acrylamide-*co*-methacryl acid)-*g*-poly(*D,L*-lactide) (P(NIPAAm-*co*-MAAc)<sub>9970</sub>-*g*-PLA<sub>6150</sub>, [NIPAAm]:[MAAc]:[PLA] = 91:6.3:2.7, with a polydispersity index (PDI) = 1.24, and a critical micelle concentration (cmc) = 1.3 mg L<sup>-1</sup>), was synthesized by traditional free-radical copolymerization from the NIPAAm monomer, the MAAC monomer and the PLA-EMA<sup>[11]</sup> (PLA with

[\*] Prof. G. H. Hsiue, Dr. C. L. Lo, C. K. Huang  
Department of Chemical Engineering, National Tsing Hua University  
101, Section 2 Kuang Fu Road, Hsinchu, 300 Taiwan (ROC)  
E-mail: ghhsie@mx.nthu.edu.tw

H. H. Chen  
Department of Applied Chemistry, National Chiao Tung University  
1001, Ta Hsueh Road, Hsinchu, 300 Taiwan (ROC)

[\*\*] C.-K.H. and C.-L.L. contributed equally. The authors thank the National Science Council of the Republic of China, Taiwan for financially supporting this work under Contract Nos. NSC 94-2320-B-007-003 and 95-2314-B-007-002. The help of the staff at the NTOU Institute of Marine Biology with TEM observation is gratefully acknowledged. TTY Biopharm Co. Ltd. (Taiwan) kindly provided the doxorubicin hydrochloride. Supporting Information is available online from Wiley InterScience or from the authors.

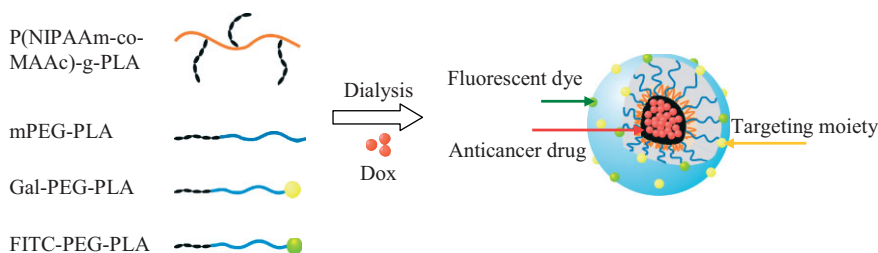


**Figure 1.** Schematic representation of multifunctional micelle structure made of a graft copolymer, a diblock copolymer and two functionalized diblock copolymers.

end-capped of ethyl methacrylated group,  $M_n$  2030) macromonomer ( $M_n$  2000) using 2,2'-azobisisobutyronitrile (AIBN) as an initiator.<sup>[12]</sup> Block I (mPEG<sub>5000</sub>-PLA<sub>530</sub>, PDI = 1.05, cmc = 84 mg L<sup>-1</sup>), Block II (mPEG<sub>5000</sub>-PLA<sub>1088</sub>, PDI = 1.15, cmc = 16 mg L<sup>-1</sup>) and Block III (mPEG<sub>5000</sub>-PLA<sub>1750</sub>, PDI = 1.20, cmc = 5.4 mg L<sup>-1</sup>) copolymers were synthesized by ring-opening polymerization from methoxy poly(ethylene glycol) (mPEG,  $M_n$  5000) and D,L-lactide using stannous octoate as a catalyst.<sup>[13]</sup> These diblock copolymers have the same chemical nature, but differ in composition ratio. Two functional end-capped diblock copolymer galactosamine (Gal)-PEG<sub>3400</sub>-PLA<sub>830</sub> (Gal-PEG-PLA, [Gal]:[PEG]:[LA] = 8.4:7.6:84) and fluorescein isothiocyanate (FITC)-PEG<sub>3400</sub>-PLA<sub>830</sub> (FITC-PEG-PLA, [FITC]:[PEG]:[LA] = 4:8:88) were synthesized by thiol-maleimide coupling reaction.<sup>[14,15]</sup> The chemical structure and PDI of each copolymer were verified by <sup>1</sup>H-NMR (AMX-500, Bruker) and GPC, using dimethylformamide (DMF) as an

elution solvent. The  $M_n$  of Graft was calculated by <sup>1</sup>H-NMR (AMX-500, Bruker) using mPEG ( $M_n$  5000) as a standard. The cmc of each copolymer was determined using a fluorescence technique with pyrene as a hydrophobic probe.<sup>[16]</sup> The final concentration of pyrene in the copolymer solution was adjusted to  $6 \times 10^{-7}$  M. The copolymer concentration varied from 0.0001 to 10 mg mL<sup>-1</sup>. Fluorescence spectra were obtained using a fluorescence spectrophotometer (F-2500, Hitachi). The excitation wavelength for the emission spectra was 339 nm and excitation spectra were recorded at 390 nm.

Before preparing multifunctional micelles, two-component mixed micelles composed of a graft copolymer and a diblock copolymer (Block I, Block II, or Block III) were employed to investigate the influence of chain length and cmc of the diblock copolymers on the morphology and structure of mixed micelles. First, a graft copolymer and a diblock copolymer were dissolved together in dimethylsulfoxide (DMSO)/dimethylformamide (DMF) (4:1 v/v) cosolvent to prepare a polymer solution. The DMF/DMSO solvent mixture was used because it produces the smallest mixed micelles. Graft copolymer concentration was fixed at 10 mg mL<sup>-1</sup>. The molar ratio of the graft copolymer to the diblock copolymer was 1:9. Mixed micelles were then prepared by dialysis against Milli-Q water using a cellulose membrane bag (molecular weight cut-off, 6000–8000; obtained from SpectrumLabs, Inc.). The Milli-Q water was re-

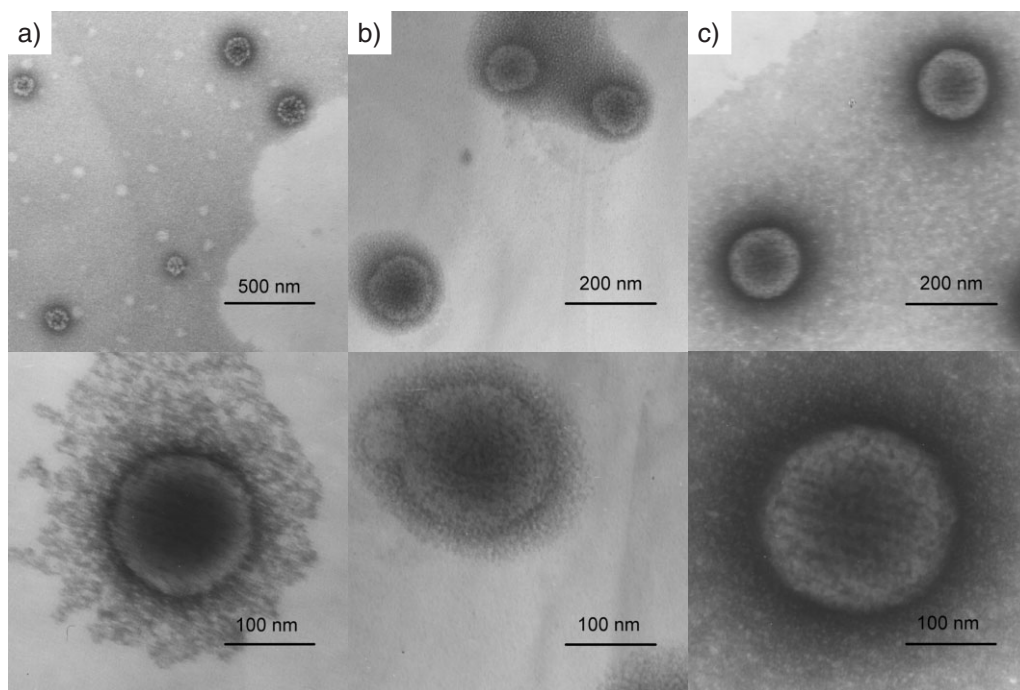


**Figure 2.** TEM images of a) mixed micelles formed from 25 mol% of graft copolymer and 75 mol% of mPEG<sub>5000</sub>-PLA<sub>530</sub>, b) mixed micelles formed from 25 mol% of graft copolymer and 75 mol% of mPEG<sub>5000</sub>-PLA<sub>1088</sub>, and c) mixed micelles formed from 25 mol% of graft copolymer and 75 mol% of mPEG<sub>5000</sub>-PLA<sub>1750</sub>. Graft copolymer concentration was fixed at 10 mg L<sup>-1</sup> in each mixed micelle before dialysis.

placed every 3 h. Graft copolymers first began to aggregate in this solvent exchange process. The hydrophobic PLA of the diblock copolymer simultaneously packed and associated to the aggregation region of the graft copolymer, forming a mixed micelle.<sup>[6,10]</sup> The core-shell structure and particle size of three mixed micelles from a graft copolymer and a diblock copolymer (Block I, Block II, or Block III) were observed by transmission electron microscopy (TEM), as shown in Figure 2. The TEM process involves staining the methacrylic acid groups of the graft copolymers using uranyl acetate (2 wt %).<sup>[17]</sup> The transmission electron micrograph was taken on a Hitachi H-600 microscope at an accelerating voltage of 100 kV. TEM observation produced three results. 1) For all mixed micelles, the dark region of the graft copolymer is the inner core, and hydrophilic segments of mPEG extended outside the core. 2) The radius of the core region decreased as the chain length of PLA of diblock copolymer increased ( $PLA_{530} > PLA_{1088} > PLA_{1750}$ ). 3) Mixed micelle particle size increased as the chain length of PLA of diblock copolymer increased ( $PLA_{1750} > PLA_{1088} > PLA_{530}$ ). A short PLA length produces smaller mixed micelles.

A basic evaluation of pharmacokinetic modeling and efficacy data for micelles or drug loaded micelles in animal models was conducted. This tested the stability of micelles or drug loaded micelles in the presence of serum or serum albumins.<sup>[18]</sup> In this study, mixed micelles (25 mol % of graft copolymer and 75 mol % of mPEG<sub>5000</sub>-PLA<sub>1750</sub>) were suspended in PBS in the presence of 4 wt % of bovine serum albumin (BSA) at 37 °C. Dynamic light scattering measurement was then used to evaluate the adsorption of BSA and its interaction with micelles. The authors used the CONTIN analytic method. The average micelle diameter before BSA treatment was measured. The ratio of the micelle diameter after BSA treatment to the initial size (before BSA treatment) indicates significant adsorption and aggregation. Results (see Supporting Information) show that mixed micelles were stable after 72 h because the hydrophilic outer shell mPEG prevented albumin adsorption on mixed micelles. This is one indication that mixed micelles could prolong the circulation after intravenous injection.

According to the results above, mixed micelles can be prepared from two or more components and can be extended for multifunctions by manipulating and carefully designing each component. A multifunctional micelle was prepared from four components, including FITC-PEG-PLA, Gal-PEG-PLA, Block III (mPEG<sub>5000</sub>-PLA<sub>1750</sub>) and graft copolymer. The graft copolymer in multifunctional micelles could encapsulate anticancer drugs and control drug release by moderating pH and temperature changes.<sup>[12]</sup> Block III in micelles helped control the core-shell structure and obtain uniform micellar distribution. The fluorescence dye conjugated diblock copolymer FITC-PEG-PLA in micelles provided direct evidence of where micelles accumulated after cell uptake. On the other hand, the targeting moiety (Gal) conjugated diblock copolymer Gal-PEG-PLA could combine with the asialoglycoprotein of HepG2 cells proceeding to the active tumor targeting.

The multifunctional micelle incorporated with Dox was also prepared using the dialysis method. First, Dox was neutralized

with a 1.2 molar excess of triethyl amine<sup>[19,20]</sup> in DMSO/DMF (4/1 v/v). This mixture was stirred to dissolve the drug. Fifty mol % of graft copolymer, 20 mol % of Block, 15 mol % of Gal-PEG-PLA, and 15 mol % of FITC-PEG-PLA were then dissolved in the drug solution. The mixture was dialyzed against Milli-Q water for 72 h using a membrane with a molecular-weight cut-off of 6000–8000 at room temperature. The Milli-Q water was replaced every 3 h. Multifunctional micelles were obtained by a freeze-drying process. The DOX loading level was about 31 wt % in weight, which was determined by a UV/Vis spectrophotometer as multifunctional micelles dissolved in DMSO. Figure 3a shows the TEM images of multifunctional micelles stained with uranyl acetate (2 wt %). These results demonstrate the integrity of the core-shell structure.

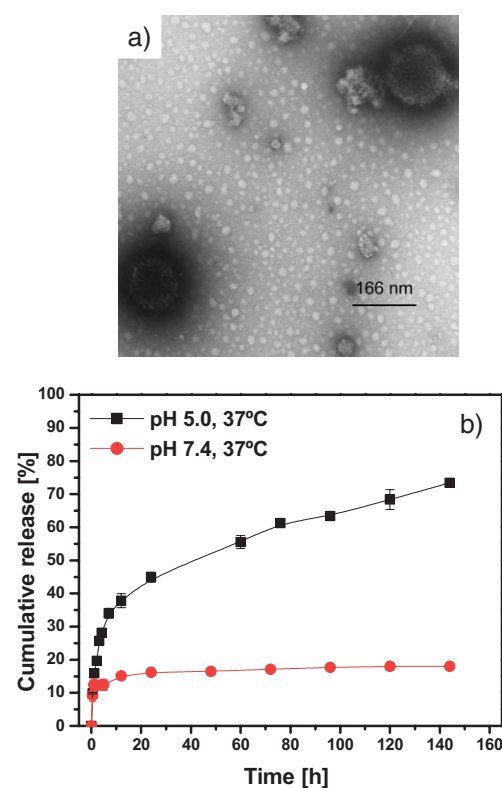


**Figure 3.** a) TEM image of multifunctional micelles. b) Release of Dox from multifunctional micelles under acidic (pH 5.0) and neutral (pH 7.4) conditions at 37 °C. Mean  $\pm$  sd ( $n=3$ ).

The multifunctional micelle particle size was approximately 160 nm. As mentioned, macromolecular transport across blood vessels has been shown to occur via open gaps (interendothelial junctions and transendothelial channels), caveolae, vesicular vacuolar organelles, and fenestrations. The pore cutoff size in most tumor studies was between 380 and 780 nm.<sup>[21]</sup> Multifunctional micelles in this study are below 200 nm, and would extravasate through the passageways described. Particle size has also been found to significantly influence the organ distribution of PEG-coated nanoparticles. A diameter of less than 200 nm is required to avoid spleen filtering effects.<sup>[22]</sup> Particle

size might also determine the internalization mechanism. Large particles (up to 500 nm) enter the cell by receptor- and clathrin-independent endocytosis while smaller particles (<200 nm) could be internalized via coated pits through a non-specific clathrin-dependent process.<sup>[23]</sup> Thus, the multifunctional micelles in this study were approximately 160 nm in size, close to the typical required size under physiological conditions.

To evaluate the effects of stimulus-response behavior on controlled drug delivery, the *in vitro* drug release behaviors of multifunctional micelles were studied in two different buffered solutions (pH 7.4 and 5.0). Figure 3b shows results. In neutral surroundings (pH 7.4), multifunctional micelles exhibited initial burst effects, losing about 15 wt % at 37 °C. Release behavior remained constant after 140 h. In acidic surroundings (pH 5.0), release behavior was obviously divided into two periods. A rapid release in the first period was followed by a sustained and slow release over a prolonged time, up to a hundred hours for physically-encapsulated intelligence drug carriers. The initial rapid release (35 wt %) was observed in the initial 2 h and followed by a sustained release for 140 h until reaching a 70 wt % release profile. The authors' previous study shows that the P(NIPAAm-*co*-MAAc) main chains of graft copolymers collapsed and aggregated under acidic conditions at 37 °C, deforming the inner core structure and showing an increase of  $I_1/I_3$  of the pyrene emission spectra.<sup>[4,12]</sup> The ratio  $I_1/I_3$ , of the first vibrational band intensity to that of the third vibrational band can then be used as an environmental polarity index.<sup>[24]</sup> A higher ratio corresponds to more polar surroundings of the pyrene probe.<sup>[25]</sup> In this case, the change in  $I_1/I_3$  of multifunctional micelles was small (see Supporting Information). This is probably because the pyrene molecules were partitioned in the hydrogen-bonding region between mPEG and MAAc in acidic conditions. However, drug release behavior results corroborate the claim that the multifunctional micelles are pH sensitive because changing the pH deformed the core structure and released Dox.

The multifunctional micelles and free Dox were tested for *in vitro* cytotoxicity using a tetrazolium dye (MTT) method. The MTT-based cytotoxic activities of the multifunctional micelles and free DOX were compared after 24 h and 72 h incubation with HeLa cells (see Supporting Information). The inhibition concentration ( $IC_{50}$ ) of multifunctional micelles was 25  $\mu\text{g mL}^{-1}$  at 24 h but decreased to 4  $\mu\text{g mL}^{-1}$  at 72 h. The cytotoxicity of multifunctional micelles at 72 h was similar free Dox ( $IC_{50} = 1.2 \mu\text{g mL}^{-1}$ ). On the other hand, the  $IC_{50}$  of empty multifunctional micelles was 792  $\mu\text{g mL}^{-1}$  after 72 h of incubation. This indicates that the cytotoxicity of HeLa cells came from the Dox released by multifunctional micelles.

To evaluate the functionality of multifunctional micelles in biomarker applications, confocal laser scanning microscopy (CLSM) was used to observe the fluorescence images of multifunctional micelles and released Dox after HeLa cells uptake. The triggering mechanism of most particulate carriers must occur in the endosome to release the drug in the cytoplasm.<sup>[3,4,12,16,19,26–29]</sup> Figure 4a shows fluorescence images of

multifunctional micelles incubated with HeLa cells for 6 h. HeLa cells showed green fluorescence in the cytoplasm, indicating that the multifunctional micelles were located there. Additionally, the released Dox, with a red fluorescence, was localized in both the cytoplasm and the nucleus. The clear distribution of where particulate carrier location was observed by the FITC-labeled micelles.

To evaluate the functionality of multifunctional micelles in specific tumor targeting, multifunctional micelles were incubated with HepG2 (hepatocellular carcinoma) cells to confirm drug cytotoxicities. Hepatocytes have large numbers of asialoglycoprotein receptors on their surface that recognize galactose residues.<sup>[30,31]</sup> Because of their specific ligand-receptor binding, the internalization of multifunctional micelles (containing the targeting moiety, Gal) into cancer cells can be performed by the receptor-mediated endocytosis process (active tumor targeting) and delivered to the lysosomes.<sup>[32]</sup> The viability (percentage of surviving cells) of HepG2 cells after 24 h and 48 h incubation was compared with multifunctional micelles. Figure 4b shows the effects of specific tumor targeting and non-specific tumor targeting of Dox-loaded micelles on receptor-mediated endocytosis. Cell viability was assessed using a direct count of 0.2% trypan blue dye exclusion assay to observe the rate of growth inhibition caused by the released Dox. For the positive control, cells were incubated at 4 °C with multifunctional micelles to allow binding (but not internalization) to occur for 2 h. They were then replaced with fresh medium and warmed to 37 °C for various length of times. For the negative control, cells were incubated at 37 °C with multifunctional micelles and underwent the same procedures as the positive control. The multifunctional micelles had lower cell viabilities than those without Gal in either positive control or negative control. This is because the multifunctional micelles bound with asialoglycoprotein and then internalized into cancer cells to release Dox by intracellular pH changes. Additionally, at 37 °C the cell viability of all cells incubated with multifunctional micelles was lower than that of the cells incubated at 4 °C, suggesting an endocytosis process and a large accumulation. Cell viability was also compared at the same Dox dosage. Free Dox exhibited more potent activity than the multifunctional micelles and mixed micelles at 4 °C, because the accumulated process of free Dox was more direct than micelles. The specific asialoglycoprotein-multifunctional micelle interactions were verified by an inhibition assay. The incubation of cells with 150 mM galactose completely abolished micelle cell binding and indicated sugar specificity of the process involved (Fig. 4c).

### 3. Conclusion

Mixed micelles encapsulating Dox were successfully prepared by dialysis, producing multifunctionalities which can be used as cancer diagnosis agents and cancer drug delivery carriers. TEM images revealed that the multifunctional micelles are spherical in shape and about 160 nm in size, which is suitable for intravenous injection and close to the typically re-



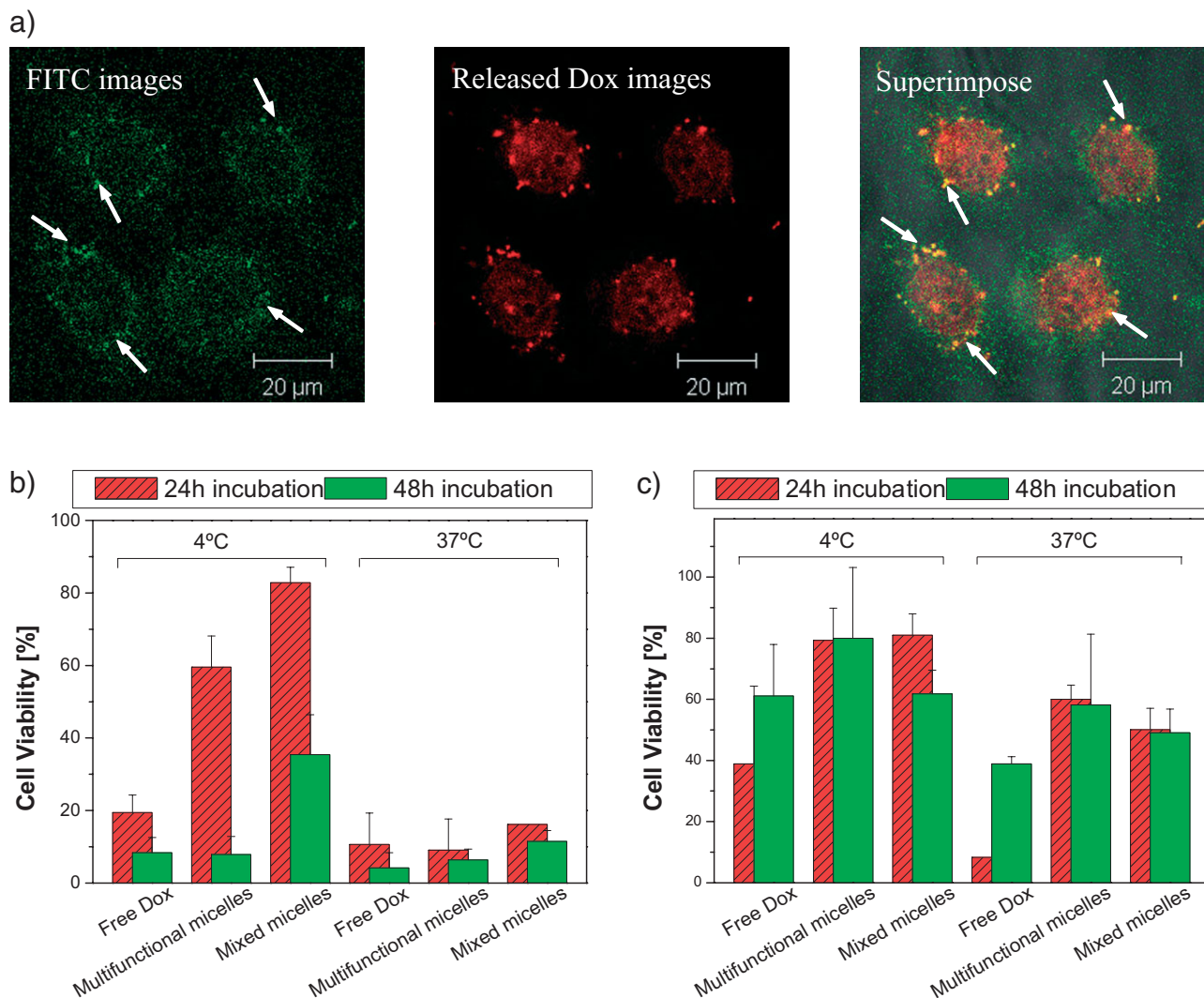


**Figure 4.** Evaluation of multifunctional micelle functionalities in drug delivery applications. a) Confocal images of HeLa cells incubated with multifunctional micelles ( $50 \mu\text{g mL}^{-1}$ ) showing the particulate distribution and localization of released Dox after 6 h internalization. Green fluorescence represents FITC-labeled multifunctional micelles, and red fluorescence represents released Dox. Arrows indicate multifunctional micelle accumulation. b) Free Dox cytotoxicity, multifunctional micelle cytotoxicity and mixed micelle cytotoxicity after incubation with HepG2 cells for 24 h and 48 h. Dox dosage was  $50 \mu\text{g mL}^{-1}$ . c) Free Dox cytotoxicity, multifunctional micelle cytotoxicity and mixed micelle cytotoxicity after incubation with HepG2 cells for 24 h and 48 h in the presence of 150 mM galactose. Dox dosage was  $50 \mu\text{g mL}^{-1}$ .

quired size under physiological conditions. Tumor targeting assay and CLSM measurements revealed that multifunctional micelles exhibited a high cytotoxicity by receptor-mediated endocytosis and showed clear fluorescence imaging of their distribution. Although Dox release behavior via intracellular pH changes and the pH and temperature characters of mixed micelles<sup>[33]</sup> were reported by our previous study, our goal here was to show a proof-of-concept: that is, producing an ideal micelle with a long circulation time, tumor recognition, and combined cancer diagnosis and controlled drug delivery for cancer therapy. In the future, multifunctional micelles combined with a near IR dye (e.g., Cy5.5) to replace FITC can be extended to animal models to evaluate the distribution in the body and cancer therapy.

#### 4. Experimental

**FITC-PEG-PLA Diblock Copolymer Synthesis:** PLA-NH<sub>2</sub>: N-Boc-L-alaninol was converted to the corresponding alkoxide (N-Boc-L-alaninol-OK) using potassium/naphthalene. D,L-lactide was then polymerized at 100 °C for 12 h using N-Boc-L-alaninol-OK as an initiator and toluene as the solvent to obtain PLA-NHBoc. The polymerization was terminated by adding acetic acid to the reaction mixture and PLA-NHBoc was precipitated from diethyl ether. The Boc group was removed from the PLA-NHBoc by treating the mixing solvent with formic acid (20 mL) and CHCl<sub>3</sub> (20 mL). After 9 h treatment at room temperature, the solution was poured into a large amount of diethyl ether to obtain the precipitate. The precipitate was vacuum dried at room temperature. The product was then treated in a mixing solvent of triethylamine (20 mL) and CHCl<sub>3</sub> (20 mL) to deprotonate at room temperature for 8 h. PLA-NH<sub>2</sub> was purified by a method similar to that for PLA-NHBoc.

**PLA-SH:** Thiolated PLA was synthesized by covalent modification of the PLA-NH<sub>2</sub> primary amino groups by adding sulhydryl moieties. For the synthesis, PLA-NH<sub>2</sub> was dissolved in acetonitrile and then incubated with an excess of 2-iminothiolane hydrochloride at room temperature for 15 h [14,15]. The unreacted 2-iminothiolane was removed by repeated dialysis against 5 mM HCl solution followed by 1 mM HCl solution for 24 h each. The purified PLA-SH was vacuum dried.

**Maleimide-PEG-NH<sub>2</sub>:** Aliquots of N-Methoxycarbonylmaleimide in dimethyl sulfoxide (DMSO) were added to an aqueous solution of polyoxyethylene bis(amine) at room temperature. The mixture was allowed to react for 6 h. After the reaction, the resulting Maleimide-PEG-NH<sub>2</sub> was purified by recrystallization from dichloromethane and diethyl ether cosolvent at -20 °C.

**PLA-PEG-NH<sub>2</sub>:** PLA-SH was dissolved in 0.1 M Tris/acetonitrile (1:3 v/v) (aq, pH 6.5, adjusted by 0.5 M NaOH solution) and then added to Maleimide-PEG-NH<sub>2</sub> Tris solution. The reaction mixture was shaken and allowed to continue for 6 h at room temperature. After the reaction, the product was purified by dialysis against PBS and Milli-Q water using a cellulose membrane bag (molecular weight cut-off, 6000–8000; obtained from SpectrumLabs, Inc.) and then frozen in a freeze dryer system (Heto-Holten A/S, Denmark) to yield dried product. The dried product was dissolved in dichloromethane and purified by precipitation from diethyl ether to remove unreacted PLA-SH. NH<sub>2</sub>-PEG-PLA was obtained under vacuum.

**FITC-PEG-PLA:** NH<sub>2</sub>-PEG-PLA was dissolved in methanol and the fluorescein isothiocyanate (FITC) was then added. The mixture was stirred for 24 h at room temperature. The reaction mixture was then dialyzed against 0.5 M NaCl solution followed by dialysis against Milli-Q water for 2 days to remove methanol solvent and unreacted small molecules. Dried FITC-PEG-PLA product was obtained by a freeze dryer system.

**Gal-PEG-PLA Diblock Copolymer Synthesis: Gal-Maleimide:** Aliquots of N-methoxycarbonylmaleimide in dimethyl sulfoxide (DMSO) were added to an aqueous solution of galactosamine hydrochloride at room temperature. The mixture was allowed to react for 6 h. The resulting Gal-Maleimide was purified by precipitation from diethyl ether.

**PLA-PEG-SH:** Thiolated PLA was synthesized by the PLA-PEG-NH<sub>2</sub> with the addition of sulhydryl moieties. For the synthesis, PLA-PEG-NH<sub>2</sub> was dissolved in acetonitrile and incubated with an excess of 2-iminothiolane hydrochloride at room temperature for 15 h. Unreacted 2-iminothiolane was removed by repeated dialysis against 5 mM HCl solution followed by 1 mM HCl solution for 24 h. The Milli-Q water was replaced every 3 h. The purified PLA-PEG-SH was vacuum dried.

**Gal-PEG-PLA:** PLA-PEG-SH was dissolved in methanol and Gal-Maleimide was then added. The mixture was stirred for 24 h at room temperature. The reaction mixture was then dialyzed against 0.5 M NaCl solution followed by dialysis against Milli-Q water for 2 days to remove methanol solvent and unreacted small molecules. The dried Gal-PEG-PLA product was obtained by a freeze dryer system.

**Transmission Electron Microscopy (TEM) Observation.** Observations of mixed micelle size and distribution employed a Hitachi H-600 microscope at an accelerating voltage of 100 kV. A drop of sample solution (~5 µL) with a 2 mg mL<sup>-1</sup> concentration was placed onto a copper grid coated with carbon, tapped with a filter paper to remove surface water, and air-dried for 5 min. Then, the grid was negatively stained with 2 wt % uranyl acetate solution, tapped with a filter paper to remove surface water, and vacuum-dried for 24 h.

**Drug Content Evaluation:** Weighted amounts of the multifunctional micelles were dissolved in DMSO at room temperature for 12 h and the ultrafiltered (ultrafiltration membrane MWCO 1000, Millipore). Samples were then removed and analyzed to determine Dox content using a UV/Vis spectrometer at 485 nm referencing a Dox calibration curve in DMSO. The Dox content in the multifunctional micelles was thus determined. The drug content of multifunctional micelles was calculated using the formula drug content (% w/w) = (total mass of Dox in mixed micelles)/(total mass of Dox in mixed micelles + total mass of polymer in mixed micelles) × 100. The drug content of mixed micelles incorporating Dox was determined by UV/Vis spectrophotometer analysis to be about 31.4 wt %.

**Drug Release Assay:** The release of multifunctional micelles in pH 5.0 and pH 7.4 buffer solutions at 37 °C was examined. Dox released from multifunctional micelles was isolated from the multifunctional micelle buffer solution (50 mg L<sup>-1</sup>) by ultrafiltration (ultrafiltration membrane MWCO 10000, Millipore). The isolated solution was measured using a UV/Vis spectrometer at 485 nm in a time-course procedure.

**Internalization:** Accumulated Dox and multifunctional micelles in HeLa cells were localized using a Carl Zeiss LSM5 PASCAL confocal laser scanning microscope (CLSM). The HeLa cells were seeded on coverslides for 24 h and then treated with free Dox or multifunctional micelles. Multifunctional micelles were washed twice with PBS to remove untrapped Dox before use. The concentration of Dox was approximately 10 µg mL<sup>-1</sup>. After an interval, the cells were washed twice with PBS and then mounted on a slide with 4 wt % paraformaldehyde for CLSM observation. Fluorescence observation was carried out with a confocal microscope at 488 nm for excitation and an LP filter of 590 nm for Dox detection. Multifunctional micelle observation was carried out with a confocal microscope at 405 nm for excitation and an appropriate filter for detection.

**Tumor Targeting Evaluation:** HepG2 cells (2 × 10<sup>4</sup> cells/mL) were seeded in a 25-T flask of DMEM medium with 10 % fetal bovine serum (FBS) in a humidified atmosphere of 5 % CO<sub>2</sub> at 37 °C. After the HepG2 cells had been incubated in a logarithmic growth phase, samples of co-culturing were added for 2 h at 4 °C. HepG2 cells were twice washed by PBS solution, and fresh medium was added for 24 h and 48 h incubation in a humidified atmosphere of 5 % CO<sub>2</sub> at 37 °C. At the end of the experiment, cell viability was calculated by trypan blue staining using a phase contrast microscopy. The same process was repeated at 37 °C through the entire process as a contrast. As above, galactose (150 mM) was also added to the system in the accepted way of performing an inhibition assay.

Received: September 6, 2006

Revised: December 30, 2006

Published online: August 8, 2007

- [1] X. Gao, Y. Cui, R. M. Levenson, L. W. K. Chung, S. Nie, *Nat. Biotechnol.* **2004**, *22*, 969.
- [2] N. Kang, M. E. Perron, R. E. Prud'Homme, Y. Zhang, G. Gaucher, J. C. Leroux, *Nano Lett.* **2005**, *5*, 315.
- [3] E. S. Lee, K. Na, Y. H. Bae, *Nano Lett.* **2005**, *5*, 325.
- [4] C. L. Lo, K. M. Lin, C. K. Huang, G. H. Hsiue, *Adv. Funct. Mater.* **2006**, *16*, 2309.
- [5] D. F. K. Shim, C. Marques, M. E. Cates, *Macromolecules* **1991**, *24*, 5309.
- [6] C. Honda, K. Yamamoto, T. Nose, *Polymer* **1996**, *37*, 1975.
- [7] A. L. Borovinskii, A. R. Khokhlov, *Macromolecules* **1998**, *31*, 7636.
- [8] C. Konak, M. Helmstedt, *Macromolecules* **2003**, *36*, 4603.
- [9] W. Mingvanisig, C. Chaibundit, C. Boot, *Phys. Chem. Chem. Phys.* **2002**, *4*, 778.
- [10] T. Liu, V. N. Nace, B. Chu, *Langmuir* **1999**, *15*, 3109.
- [11] J. A. Wallach, S. J. Huang, *Biomacromolecules* **2000**, *1*, 174.
- [12] C. L. Lo, K. M. Lin, G. H. Hsiue, *J. Controlled Release* **2005**, *104*, 477.
- [13] T. Riley, S. Stolnik, C. R. Heald, C. D. Xiong, M. C. Garnett, L. Illum, S. S. Davis, *Langmuir* **2001**, *17*, 3168.
- [14] T. P. King, Y. Li, L. Kochoumian, *Biochemistry* **1978**, *17*, 1499.
- [15] S. Kommareddy, M. Amiji, *Bioconjugate Chem.* **2005**, *16*, 1423.
- [16] G. H. Hsiue, C. H. Wang, C. L. Lo, C. H. Wang, J. P. Lin, J. L. Yang, *Int. J. Pharm.* **2006**, *317*, 69.
- [17] S. Kwon, J. H. Park, H. Chung, I. C. Kwon, S. Y. Jeong, *Langmuir* **2003**, *19*, 10188.
- [18] P. Opanasopit, M. Yokoyama, M. Watanabe, K. Kawano, Y. Maitani, T. Okano, *J. Controlled Release* **2005**, *104*, 313.
- [19] K. S. Soppimath, D. C. W. Tan, Y. Y. Yang, *Adv. Mater.* **2005**, *17*, 318.
- [20] F. Kohori, M. Yokoyama, K. Sakai, T. Okano, *J. Controlled Release* **2002**, *78*, 155.
- [21] S. K. Hobbs, W. L. Monsky, F. Yuan, W. Gregory Roberts, L. Griffith, V. P. Torchilin, R. K. Jain, *Proc. Natl. Acad. Sci. USA* **1998**, *95*, 4607.

- [22] S. M. Moghimi, C. J. H. Porter, I. S. Muir, L. Illum, S. S. David, *Biochem. Biophys. Res. Commun.* **1991**, *177*, 861.
- [23] S. Simoes, P. Pedro, N. Duzgunes, M. Pedrosa de Lima, *Curr. Opin. Mol. Therapeut.* **1999**, *1*, 147.
- [24] K. Kalyanasundaram, T. K. Thomas, *J. Am. Chem. Soc.* **1977**, *99*, 2039.
- [25] A. L. Kjøniksen, B. Nyström, H. Tenhu, *Colloids Surf. A* **2003**, *228*, 75.
- [26] K. Vogel, S. Wang, R. J. Lee, J. Chmielewski, P. S. Low, *J. Am. Chem. Soc.* **1996**, *118*, 1581.
- [27] Y. J. Rui, S. Wang, P. S. Low, D. H. Thompson, *J. Am. Chem. Soc.* **1998**, *120*, 11 213.
- [28] Y. Bae, S. Fukushima, A. Harada, K. Kataoka, *Angew. Chem. Int. Ed.* **2003**, *42*, 4640.
- [29] E. R. Gillies, T. B. Jonsson, J. M. J. Frechet, *J. Am. Chem. Soc.* **2004**, *126*, 11 936.
- [30] A. L. Schwartz, S. E. Fridovich, H. F. Lodish, *J. Biol. Chem.* **1982**, *257*, 4230.
- [31] A. L. Schwartz, A. Bolognesi, S. E. Fridovich, *J. Cell Biol.* **1984**, *98*, 732.
- [32] R. Fallon, A. L. Schwartz, *Adv. Drug Delivery Rev.* **1989**, *4*, 49.
- [33] C. L. Lo, C. K. Huang, K. M. Lin, G. H. Hsiue, *Biomaterials* **2007**, *28*, 1225.
-